

New Approach to Discriminate Surface Dynamics and Atmospheric Effects in Single INSAR Pair

Alexander Zakharov, Kotelnikov' FIRE RAS, 141190 Vvedensky square, 1, Fryazino, Moscow region, Russia
E-mail: aizakhar@sunclass.ire.rssi.ru

Abstract

Atmospheric heterogeneities are serious corrupting effect in SAR observations, as they lead to variations of SAR signal path length. Respective phase variations on SAR interferograms preclude correct estimations of phase describing Earth surface dynamics. Various techniques of the atmospheric distortions reduction were proposed last years. They are based mostly on averaging the stacks of interferograms or incorporation of external measurements of atmosphere spatial properties. In our report we propose new approach to discriminate surface dynamics and atmospheric effects on a single INSAR pair, which does not require external information about the heterogeneities.

1 Introduction

Variations of atmosphere properties like as water vapor content in troposphere or total electron content in ionosphere lead to variations of signal path length and respective deviations of phase on SAR interferograms. In the case of ground deformation studies by means of repeated orbits SAR interferometry such a deviations introduce errors in measurements of the effect of interest. Many techniques allowing the reduction or cancellation of atmospheric distortions were proposed last time. An averaging the stacks of interferograms with statistically independent atmospheric errors is proposed, for example, in [1]. Other approaches are based on utilization of external information about atmosphere allowing the compensation of atmospheric errors on interferograms such as GPS measurements [2], MERIS [3], MODIS [4], as well as models of atmosphere [5], including selection of cloud-free observations, when troposphere impact is reduced significantly [6].

2 Atmospheric Heterogeneities

Most important for INSAR studies atmospheric effects are caused by ionospheric and tropospheric irregularities or heterogeneities. Manifestation of ionospheric irregularities was observed firstly in 90-ies in C-band on ERS SAR images. They are more prominent in L-band. Quiet ionosphere may be characterized by total electron content (TEC) about 10^{17} m^{-2} with maximal electron concentration in F-layer at 30050-400 km altitude. Ionosphere irregularities are 3% of TEC in quiet case and may reach few tens % in disturbed case. Monotonous variations of TEC along the synthesized aperture lead to the displacements of SAR image segments in azimuth direction. The displacements of the image segments were revealed during interferometric

processing on the coregistration maps in a form of azimuth streaks, which may corrupt the interpretation of surface dynamics nature, especially in the areas of fast flows of large surface patches like as glaciers. Because of large-scale size an impact of these irregularities may be corrected effectively with phase gradient algorithms [7].

Variations of water vapor content in troposphere are another corrupting factor. Having spatial scale from first hundreds of meters to tens of kilometers they introduce additional signal path length up to 2-4 cm independently of carrier frequency. The value is dependent on meteorological conditions such as air wetness, temperature and clouds type. Both ionospheric and tropospheric heterogeneities are uncorrelated on SAR data comprising INSAR pair.

3 INSAR phase components

SAR interferometry technique has been successfully developed over past 20 years. The idea of the technique is given in detail in many publications (see, for example [8]). As it is known, phase difference on the interferogram $\Delta\varphi = \varphi_1 - \varphi_2$ depends on the following components:

$$\Delta\varphi = \Delta\varphi_t + \Delta\varphi_d + \Delta\varphi_a + \Delta\varphi_n + \Delta\varphi_0 \quad (1)$$

First of all, there is topographic phase difference, which is tied to topography variations Δh as:

$$\Delta\varphi_t = -\frac{4\pi l_p \Delta h}{\lambda r \text{tg} \alpha} \quad (2)$$

where λ - signal wavelength, r - slant range from radar till surface point, α - incidence angle, l_p - perpendicular component of interferometer baseline.

Component $\Delta\varphi_a$ describes variations of radar signal path length in the atmosphere. The component is a severe disturbing factor in the radar interferometry. There are various techniques allowing the correction of atmospheric component, but the easiest one is to work with radar data affected by atmospheric irregularities in least extent. For example, tropospheric inhomogeneities are typically small in a clear skies weather conditions. Presence or absence of significant interfering ionospheric irregularities can also be predicted using various indices of ionospheric disturbances. Anyway, usually it is impossible to avoid the atmospheric corruptions in such an easy way.

Component $\Delta\varphi_d$ characterizes shift of the reflecting surface in radial direction, along the slant range line. Extraction of component $\Delta\varphi_d$, which describes dynamics of the underlying surface during time interval between radar observations, is the task of differential radar interferometry. Phase difference $\Delta\varphi_d$ is tied to the variation of slant ranges differences Δr_d caused by surface displacements by the next relationship:

$$\Delta\varphi_d = -\frac{4\pi}{\lambda} \Delta r_d. \quad (4)$$

The component $\Delta\varphi_0$ in (1), which is unknown systematic bias in the surface dynamics studies, may be estimated using signal of stable surfaces and subsequently compensated.

4 Discrimination Technique

The idea of discrimination between atmospheric effects and surface dynamics may be illustrated on a **Figure 1**, where SAR is moving with velocity V in azimuth direction x at the altitude H above the imaged surface. For sake of simplicity we will not involve SAR observation angle into consideration and discuss imaging geometry in a projection to orbital plane, and do not take into account planet rotation.

The atmospheric irregularity on the **Figure 1**, affecting the SAR signal path length, is located at the altitude h . If we synthesize SAR image at zero Doppler, the edge of the irregularity well be located at the point A on the interferogram of the imaged surface. If being imaged from different points of orbit, the irregularity well be seen at different azimuth locations on the interferogram. If we compare interferograms synthesized at Doppler frequencies $\pm 0.25f_{rep}$ with subapertures S_1 and S_2 with length $L/2$ (L is full aperture length), then total parallax $2P=A_1A_2$ of the irregularity on the interferogram will be

$$2P = \frac{Lh}{2H} = \frac{h\lambda}{2D} \quad (5)$$

where D - length of SAR antenna.

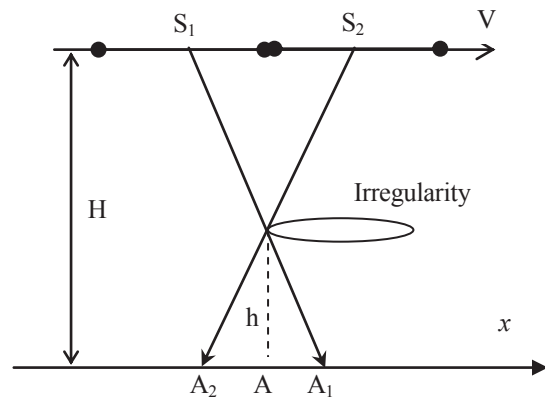


Figure 1: Parallax of atmospheric irregularity.

For L-band SAR system with 10 m antenna length total parallax will be as large as 35 m. The shorter wavelength the lower displacements will be if other things being equal.

The parallax estimation procedure should start from synthesis of two image datasets at different Doppler frequencies, say $\pm 0.25f_{rep}$ with subapertures length $L/2$ and generation of two interferograms I_1 and I_2 . Images P_1 and P_2 coregistration is necessary to remove images mutual displacements because of the fact they were generated at different Doppler frequencies. It is necessary to underline that on the coregistered interferograms I_1 and I_2 patterns describing surface dynamics will coincide. Patterns caused by atmosphere irregularities will be displaced at the distance of total parallax $2P$, which may be measured in correlation procedure. An important thing to mention is that topographic phase $\Delta\varphi_t$ in (1) should be removed preliminarily, at the stage of interferograms generation.

5 Test Area

To analyze efficiency of discrimination technique described above we use PALSAR images of Volga river estuary (North Caspian region). On the **Figure 2** below an amplitude image of the Caspian coast is presented. Respective interferogram of the area is placed on **Figure 3**.

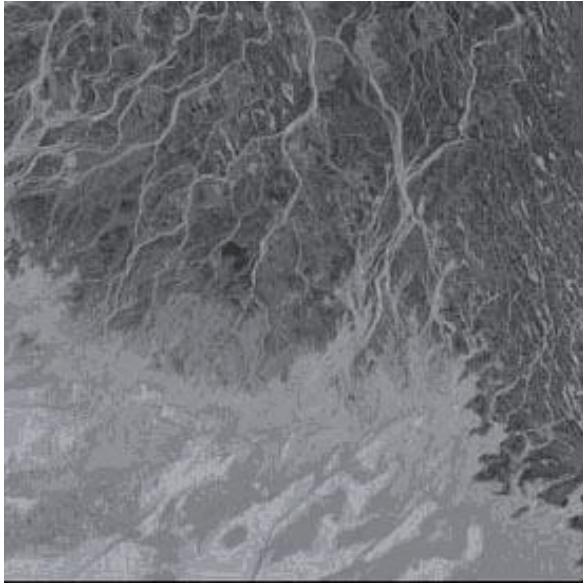


Figure 2: Amplitude image of the test area.

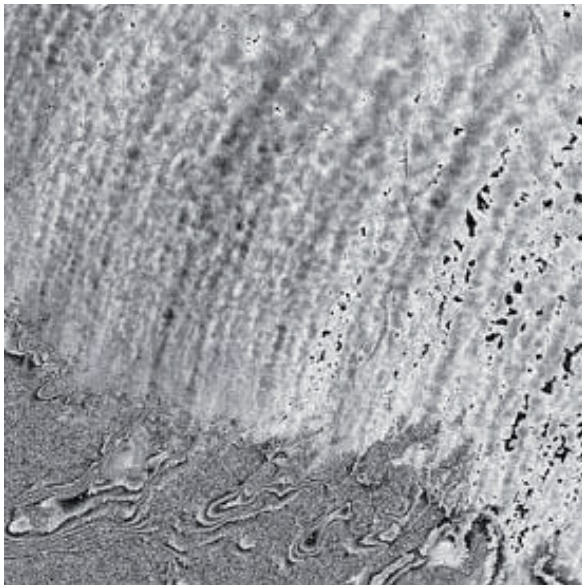


Figure 3: Interferogram of the test area.

Tropospheric heterogeneities on the interferogram of flat coastal area are clearly seen in a form of curvilinear rows. Size of spots comprising the rows is about 0.5-3 km. The respective variations of phase are about 0.3π . Good correlation of the interferograms allow the estimation of mutual displacements of atmospheric phase patterns on the interferograms generated at different Doppler frequencies and to estimate elevation of the heterogeneities on the one side and to discriminate between atmospheric patterns and surface displacement patterns on the interferogram.

6 Conclusions

The discrimination of surface dynamics and atmospheric phase patterns is possible even if the only

INSAR pair available. Atmospheric phase patterns located at non-zero altitude will be displacing on the interferograms generated at non-zero Doppler frequency compared with zero Doppler. The displacement or parallax allows the estimation of the atmospheric irregularity altitude.

References

- [1] A. Ferretti, et al: *Permanent Scatterers in SAR Interferometry*, IEEE Transactions On Geoscience and Remote Sensing, vol. 39, no. 1, 2001.
- [2] C. Xu, et al: *InSAR tropospheric delay mitigation by GPS observations: A case study in Tokyo area*, Journal of Atmospheric and Solar-Terrestrial Physics 68, pp. 629–638, 2006.
- [3] Z. Li, et al: *Interferometric synthetic aperture radar atmospheric correction: Medium Resolution Imaging Spectrometer and Advanced Synthetic Aperture Radar integration*, Geophysical Research Letters, vol. 33, L06816, doi:10.1029/2005GL025299, 2006.
- [4] Z. Li, et al: *Interferometric synthetic aperture radar (InSAR) atmospheric correction: GPS, Moderate Resolution Imaging Spectroradiometer (MODIS), and InSAR integration*, Journal of Geophysical Research, vol. 110, B03410, doi:10.1029/2004JB003446, 2005.
- [5] J. Foster, et al: *Mitigating atmospheric noise for InSAR using a high resolution weather model*, Geophysical Research Letters, vol. 33, L16304, doi:10.1029/2006GL026781, 2006.
- [6] A.I.Zakharov, et al: *Earth Surface Subsidence in the Kuznetsk Coal Basin Caused by Manmade and Natural Seismic Activity According to ALOS PALSAR Interferometry*, IEEE Journal of Selected Topics in Applied Earth Observations and Remote Sensing, vol. 6, Issue 3, pp. 1578 – 1583, 2013.
- [7] D. Wahl: *Phase Gradient Autofocus — A Robust Tool for High Resolution SAR Phase Correction*, IEEE Transactions on Aerospace and Electronic Systems, vol. 30, no. 3, pp. 827-834, 1994.
- [8] P. A. Rosen, et al: *Synthetic Aperture Radar Interferometry*, Proceedings of IEEE, vol. 88, no. 3, March 2000.